

Novel Superhydrophobic Copper Mesh-Based Centrifugal Device for Edible Oil–Water Separation

Fengzhen Zhang,^{*,†} Ranhao Wu,[†] Huanhuan Zhang, Yuling Ye, Zhong Chen, and Aiai Zhang^{*}

Cite This: *ACS Omega* 2024, 9, 16303–16310

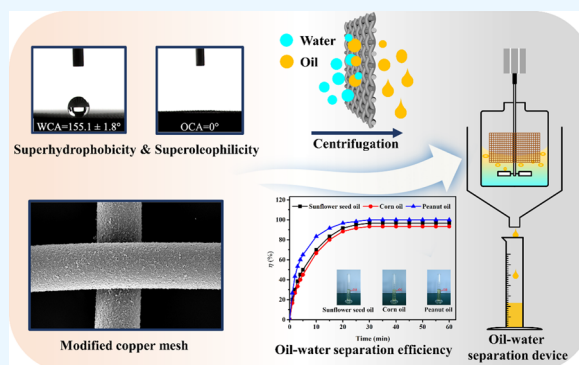
Read Online

ACCESS |

Metrics & More

Article Recommendations

ABSTRACT: Edible oil is essential for people's daily life but also results in a large amount of oily wastewater simultaneously. Oil–water separation is a practical route that can not only purify wastewater but also recycle valuable edible oil. In this study, the superhydrophobic copper mesh (SCM) was prepared by chemical etching, and a novel oil–water centrifugal device was designed for high-efficiency separation of edible oil wastewater. The kernel is a self-prepared SCM, which has a water contact angle (WCA) of $155.1 \pm 1.8^\circ$ and an oil contact angle (OCA) of 0° . Besides, the separation performance of the SCM for edible oil–water mixtures was studied in this study. The results showed that the SCM exhibited excellent oil/water separation performance, with a separation efficiency of up to 96.7% for sunflower seed oil–water wastewater, 93.3% for corn oil–water wastewater, and 98.3% for peanut oil–water wastewater, respectively. Moreover, the separation efficiency was still over 90% after 18 cycles. A model was established to analyze the oil–water separation mechanism via centrifugation. The oil–water centrifugal separation device has great potential for scale-up applications.



1. INTRODUCTION

Edible oil is an important part of the human diet, providing energy, lipid-soluble vitamins, and fatty acids. During the production of edible oil from economic crops, such as peanuts, soybeans, and sunflower seeds, a large amount of oily wastewater is produced. If the oily wastewater is directly discharged, it would cause great harm to the environment due to its high chemical oxygen demand (COD) and high biological oxygen demand (BOD). It is necessary to treat such oily wastewater to comply with environmental standards.¹ Additionally, if the oily wastewater is separated and the waste oil is utilized effectively as a raw material for biomass energy production, not only does this protect the environment but also achieves the maximum resource utilization of oily wastewater.²

The main treatment methods for oily wastewater include physiochemical treatment³ and biological treatment.⁴ Physiochemical treatment has the advantages of simple operation and short treatment time but also has disadvantages such as high cost and high energy consumption. Typical physiochemical treatment methods include adsorption,^{5,6} coagulation-flocculation,^{7,8} and electrocoagulation.^{9,10} Zhang et al.¹¹ treated acidic oily wastewater by the flocculation method and achieved a 91% oil removal rate when the dosage of flocculant P(MMA–MAA–CS)-2 was higher than 200 mg L⁻¹. However, this high flocculant dosage would make the process high cost. Sharma et al.¹² treated canola oil refinery

effluent by electrocoagulation with a COD removal rate of 93.45% at a current density of 7.61 mA cm⁻² and 40 min operation. However, the electrocoagulation method requires a high power consumption. Biological treatment decomposes complex organic matter in oily wastewater into simple substances. Although this treatment is highly adaptable and low cost, it also has the disadvantage of a long processing time. Typical biological treatments include the activated sludge method¹³ and the biofilm method.^{14,15} For example, Gonzalez et al.¹⁶ treated olive mill wastewater by a microbiological method, achieving 90% polyphenol reduction after 7 days, a much longer duration than physiochemical treatment.

Recently, superhydrophobic materials prepared by etching,^{17,18} electrochemical deposition,^{19,20} spraying,^{21,22} and hydrothermal methods^{23,24} have found good industrial applications due to their special functions such as self-cleaning and scale inhibition.²⁵ Oil–water separation is a typical application example of superhydrophobic materials.²⁶ Because of the polarity difference between oil and water, the

Received: December 28, 2023

Revised: February 25, 2024

Accepted: February 29, 2024

Published: March 29, 2024



superhydrophobic material surface attracts oil and repels water, thereby achieving oil–water separation. Oil–water separation by superhydrophobic materials has the advantage of high separation efficiency. Zhang et al.²⁷ used a superhydrophobic aluminum mesh prepared by laser etching to separate a dichloromethane–water mixture with a separation efficiency of 99%. Qiao et al.²⁸ prepared a superhydrophobic copper mesh by chemical etching and achieved the separation of a carbon tetrachloride–water mixture with a separation efficiency of 97%. However, the above separation methods were driven by gravity to separate oils with densities higher than that of water, with the superhydrophobic mesh installed at the bottom of the separation device. The probability of contact with the superhydrophobic mesh would be reduced for oils that are less dense than water (such as edible vegetable oils with a density of less than 1 g cm^{-3}); therefore, the high separation efficiency of the oil–water mixture cannot be achieved in a limited time. Lee et al.²⁹ used a superhydrophobic stainless steel mesh to separate a gasoline–water mixture and the separation efficiency was only 80%. In addition, studies have shown that superhydrophobic surfaces have been widely used in versatile applications, but the poor mechanical stability of low surface energy polymers severely limits their practical application. The inorganic hydrophobic materials have become an ideal material for the practical application of superhydrophobic surfaces.^{30–35}

Comprehensive consideration, superhydrophobic copper mesh (SCM) was prepared by chemical etching due to low equipment cost, simple process, and high controllability, and a novel oil–water separation device was designed to achieve the high separation efficiency of edible oil–water mixtures driven by centrifugation in this study. This study provides a basis for process parameter optimization and equipment design for oil–water separation.

2. EXPERIMENTAL SECTION

2.1. Materials. Copper mesh was purchased from Anping Kangmeilong Metal Mesh Co., Ltd. 1-Dodecanethiol was purchased from Shanghai Aladdin Biochemical Technology Co., Ltd. Sodium hydroxide, ammonium persulfate, anhydrous ethanol, and hydrochloric acid were purchased from Chengdu Chron Chemical Co., Ltd. All reagents were of analytical grade and were used without further processing. Deionized water was used in all of the experiments.

2.2. Preparation of SCM. The SCM was prepared by chemical etching. First, the copper mesh was sequentially cleaned with anhydrous ethanol, deionized water, and a solution of hydrochloric acid (0.1 M) with an ultrasonic cleaner (SM-5200DTD) to remove organic matter and native oxide on the copper mesh surface. The cleaned copper mesh (CCM) was then etched by a mixed aqueous solution of ammonium persulfate (0.13 M) and sodium hydroxide (2.5 M) at $60 \text{ }^\circ\text{C}$ for 20 min. After that, the etched copper mesh (ECM) was washed with deionized water and dried at $60 \text{ }^\circ\text{C}$ for 30 min. Finally, the ECM was modified by an ethanolic solution of 1-dodecanethiol (0.03 M) for 1 h at room temperature. The SCM was prepared after being washed with deionized water and dried at $60 \text{ }^\circ\text{C}$ for 30 min.

2.3. Characterization. The surface morphology of the copper mesh was observed by scanning electron microscopy (SEM; Apreo S, Thermo Scientific, USA). The phase composition of the copper mesh was analyzed by X-ray diffractometry (XRD; D2 PHASER, Bruker, USA). The surface

chemical composition of the copper mesh was determined by energy-dispersive X-ray spectroscopy (EDS; 410-M, Bruker, USA), Fourier transform infrared spectrometry (FTIR; Nicolet 6700, Thermo Scientific Company, USA), and X-ray photoelectron spectroscopy (XPS; Axis Ultra^{DLD}, KRATOS, UK). The water contact angle (WCA) and oil contact angle (OCA) were measured using a contact angle meter (JC2000D, Shanghai Zhongchen Digital Technic Apparatus Co., Ltd., China).

2.4. Oil–Water Separation Experiment. The novel self-made oil–water separation device driven by centrifugation is shown in Figure 1. The separation device mainly comprised an

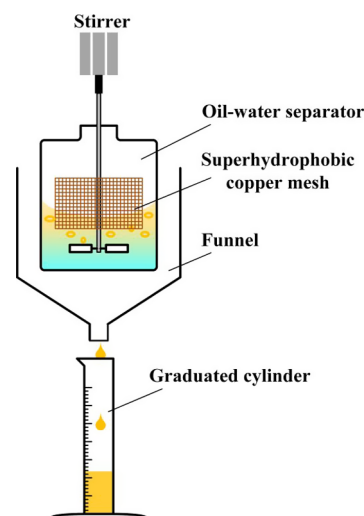


Figure 1. Self-made oil–water separation device.

oil/water separator, stirring device, and oil collection funnel. The diameter and height of the separator were 75 and 160 mm, respectively. There was a $60 \times 50 \text{ mm}$ window on the side wall, 40 mm from the bottom, with the SCM attached to this window. The stirring device provided a blade-pitch-type impeller with a diameter of 50 mm.

In each experiment, an oil–water mixture (30 mL of oil and 170 mL of water) was added to the oil–water separator. Then, the stirring device was turned on at a certain stirring speed, and the timing began. Under centrifugation, the oil was thrown out into the oil collection funnel through the SCM and then flowed into the measuring cylinder through the oil outlet at the bottom of the oil collection funnel. The volume of liquid (V_L) in the graduated cylinder was measured at different times.

3. RESULTS AND DISCUSSION

3.1. Chemical Characterization. Figure 2a shows the XRD patterns of CCM (black line), ECM (red line), and SCM (blue line). The XRD of the CCM showed the three diffraction peaks at 43.3° , 50.4° , and 74.1° , which corresponded to the (111), (200), and (220) crystalline phases of the Cu (PDF#04-0836). The ECM XRD pattern contained two new diffraction peaks at 35.5° and 38.7° , which corresponded to the (002) and (111) crystalline phases of CuO, respectively (PDF#45-0937). This indicated that CuO formed on the surface of ECM following its oxidation by the mixed aqueous solution of 0.13 M ammonium persulfate and 2.5 M sodium hydroxide at $60 \text{ }^\circ\text{C}$. The diffraction peaks on the surface of the SCM were consistent with ECM, which indicated that CuO was also present on the SCM surface.

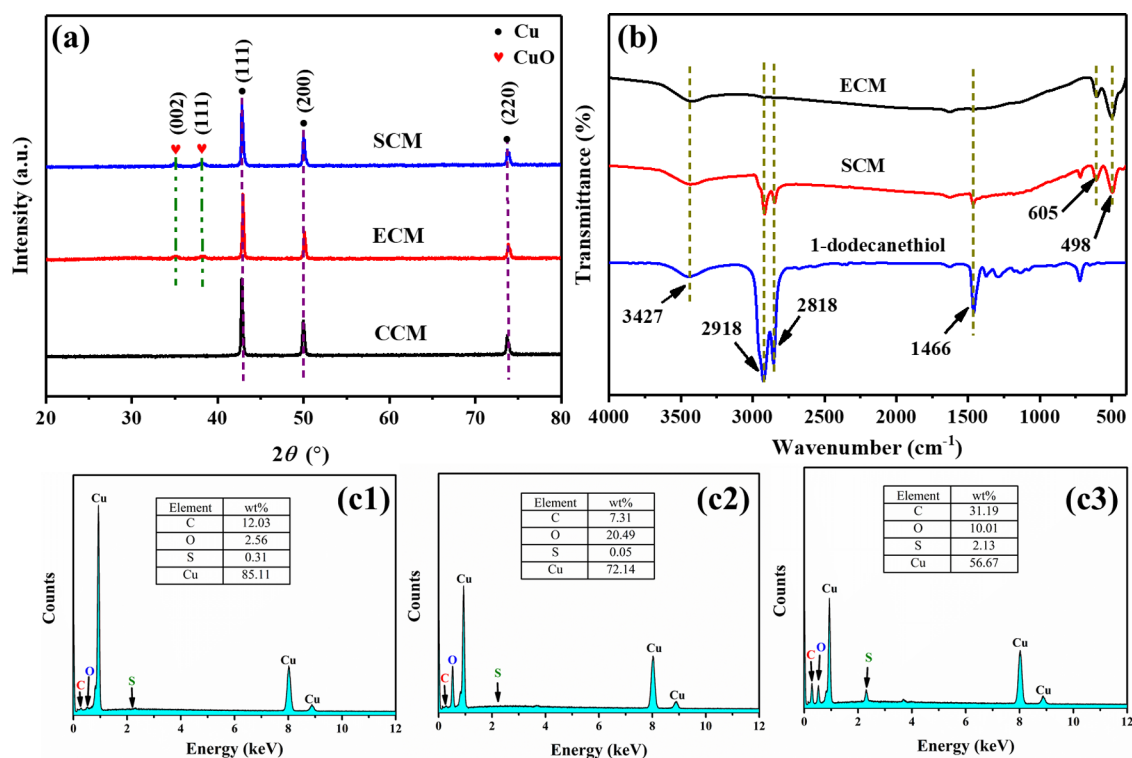


Figure 2. (a) XRD patterns of CCM, ECM, and SCM; (b) FTIR spectra of 1-dodecanethiol, SCM, and ECM; (c) EDS spectra of CCM, ECM, and SCM.

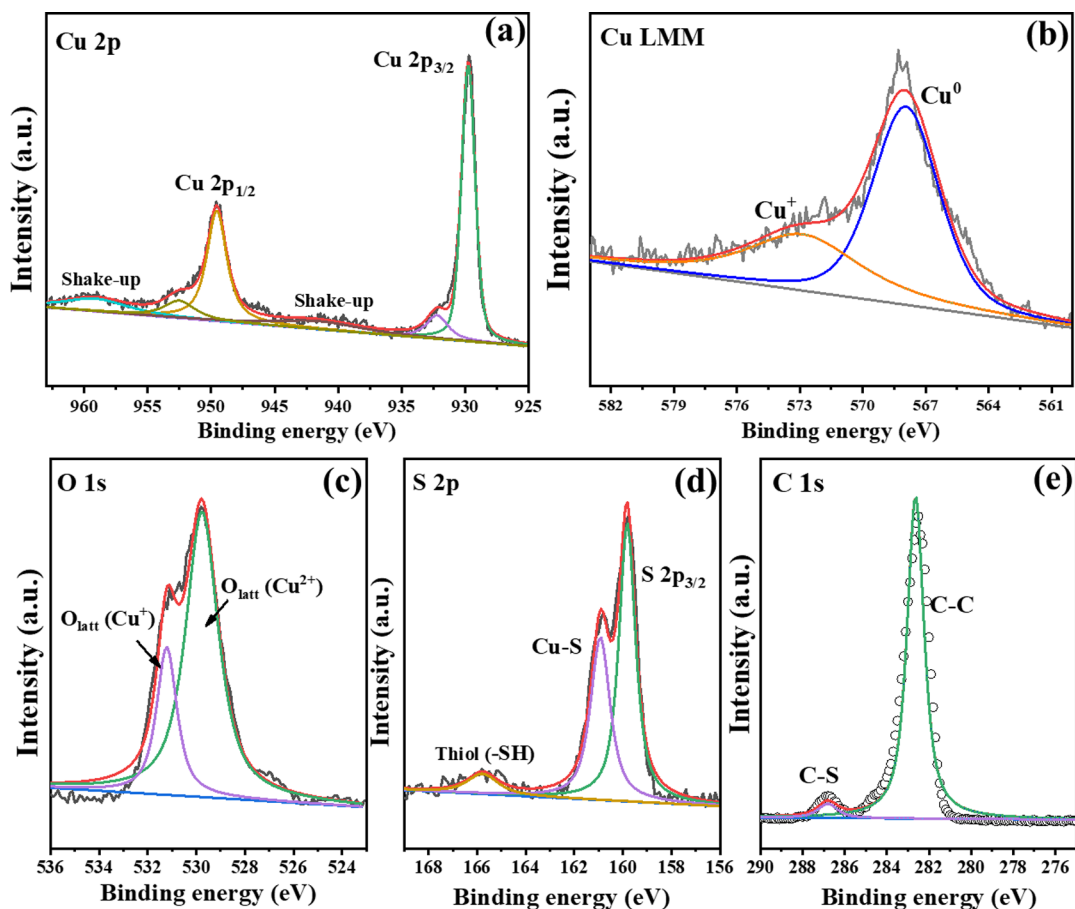


Figure 3. XPS spectra of SCM: (a) Cu 2p, (b) Cu LMM, (c) O 1s, (d) S 2p, and (e) C 1s.

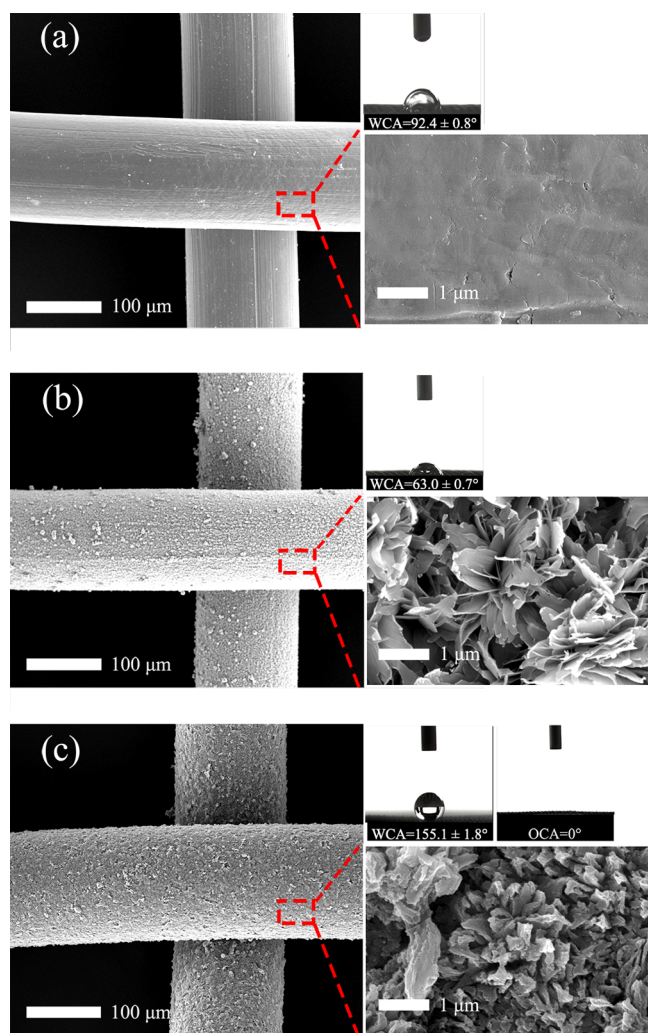


Figure 4. SEM images and WCAs of (a) CCM, (b) ECM, and (c) SCM.

The FTIR spectra of 1-dodecanethiol (blue line), SCM (red line), and ECM (black line) are shown in Figure 2b. Both ECM and SCM contained absorption peaks at 498 and 605 cm^{-1} ; these were attributed to the stretching vibration peaks of Cu–O,³⁶ which was consistent with the XRD results. The FTIR spectra of both 1-dodecanethiol and SCM showed absorption peaks at 1466 cm^{-1} , corresponding to the –S–C– stretching vibration,³⁷ as well as 2848 and 2918 cm^{-1} for the C–H stretching vibrations of –CH₂– and –CH₃, respectively.^{37,38} These FTIR spectra indicated that 1-dodecanethiol was bound to the SCM surface.

To further analyze the elemental content, EDS spectroscopy and elemental analysis of the surface of CCM (c1), ECM (c2), and SCM (c3) were performed (Figure 2c). The O content of the ECM and SCM was significantly greater than that of the CCM. In combination with the XRD pattern shown in Figure 2a, this confirmed the presence of CuO on the surface of both the ECM and SCM. Compared with the CCM and ECM, the S and C content of the SCM increased significantly. This confirmed the successful modification with 1-dodecanethiol.

To determine the composition and bonding state of the SCM surface, high-resolution XPS of Cu 2p, S 2p, and C 1s was performed (Figure 3). As shown by Cu 2p spectra in Figure 3a, the peaks at 929.7 and 949.7 eV corresponded to Cu

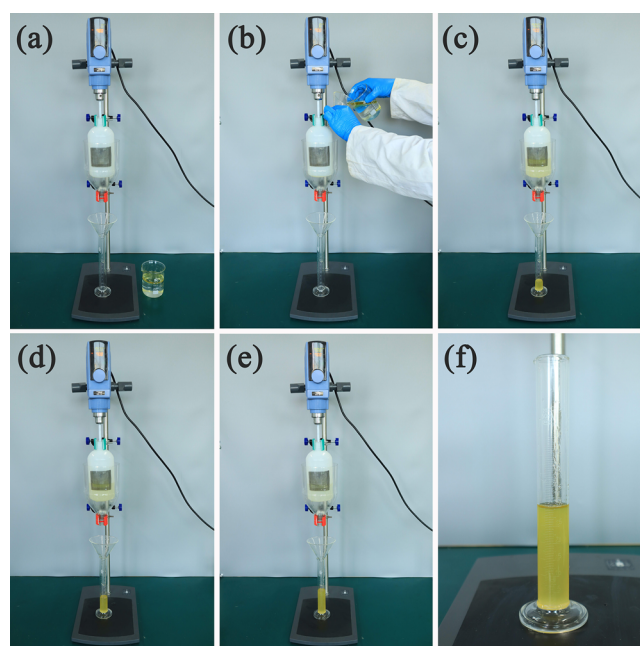


Figure 5. Separation of a peanut oil–water mixture by the self-made oil–water separation device at (a) experiment preparation; (b) pouring oil–water mixture in separation device; separation oil–water mixture at (c) 2, (d) 5, (e) 15 min, and (f) finish.

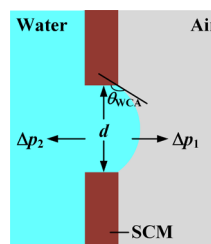


Figure 6. Schematic diagram of a water drop hanging sideways on the SCM aperture diameter (d).

Table 1. Experimental Conditions for Oil–Water Separation

experimental conditions	units	value
experimental temperature (T)	K	293.15
density of water (ρ_w)	kg m^{-3}	998.2
surface tension of water (γ_w)	mN m^{-1}	72.6
contact angle of water (θ_{WCA})	$^\circ$	155.1
diameter of the separator (D)	mm	75

$2p_{3/2}$ and Cu $2p_{1/2}$, respectively; the satellite peaks appeared at about 943.2 and 960.1 eV.³⁹ This result is indicative of the presence of CuO on the SCM surface, which is consistent with XRD results. Furthermore, the Auger electron spectroscopy for Cu LMM was carried out in Figure 3b, where the Cu LMM demonstrates the predominant role of metallic Cu⁰ species and a small amount of reduced Cu⁺ on the surface of sample.⁴⁰ The O 1s spectra (Figure 3c) can be deconvoluted into two peaks. Based on the literature data,⁴¹ the peaks at 529.1 and 531.2 eV can be attributed to the lattice oxygen of CuO ($O_{\text{latt}}(\text{Cu}^{2+})$) and lattice oxygen of Cu₂O ($O_{\text{latt}}(\text{Cu}^+)$). As for S 2p (Figure 3d), the spin–orbit peaks were correlated with the S $2p_{3/2}$ and Cu–S states, while the other obvious peaks at 165.7 eV could be ascribed to thiol (–SH) species. Specifically, the peak at 159.7 eV corresponded to the presence of S in free 1-

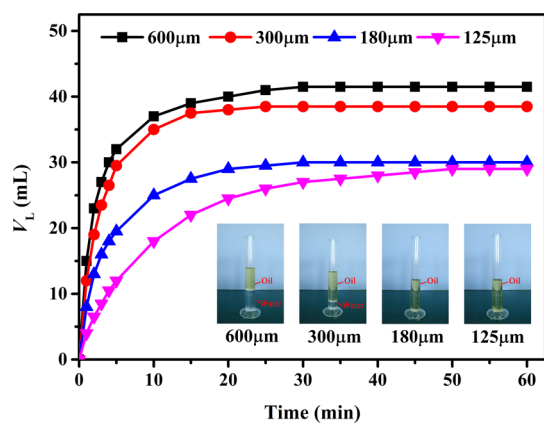


Figure 7. Effect of the SCM aperture diameter on the separation of a peanut oil–water mixture at a stirring speed of 700 rpm.

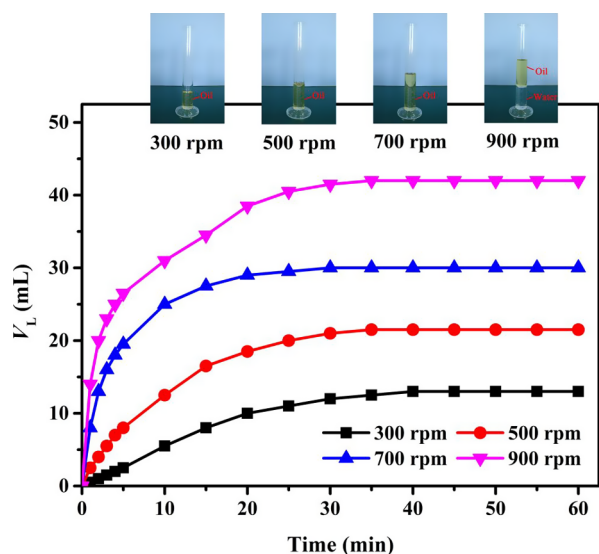


Figure 8. Effect of the stirring speed on the separation of a peanut oil–water mixture with an SCM aperture diameter of 180 μm .

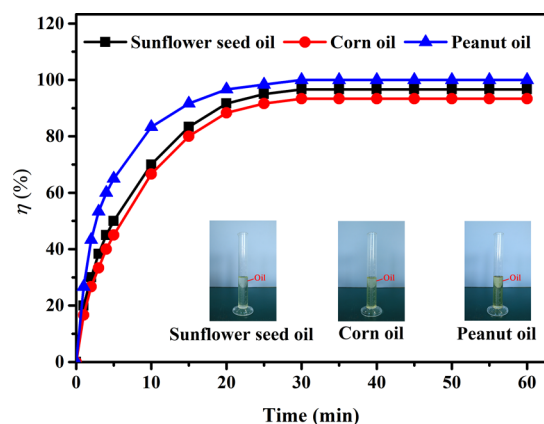


Figure 9. Separation efficiency of various edible oil–water mixtures with a stirring speed of 700 rpm and an SCM aperture diameter of 180 μm .

dodecethiol, while the peak at 161.1 eV indicated the formation of Cu–S species due to chemical bonding between S and Cu to form $\text{Cu}(\text{SC}_{12}\text{H}_{25})_2$.⁴² Furthermore, the C 1s XPS spectra in Figure 3e were deconvoluted into two peaks at 282.6

eV (C–C) and 286.9 eV (C–S), which can be ascribed to carbon atoms present in aliphatic chain and carbon bonded to sulfur originating from 1-dodecanethiol.⁴³ The XPS results demonstrated that 1-dodecanethiol effectively modifies the SCM through partial chemical bonding and simultaneously oxidizes the SCM during the etching process, which is in agreement with FTIR and EDS results.

3.2. Surface Morphology and Wettability of Copper Mesh. Figure 4 shows the SEM and WCA images of the CCM, ECM, and SCM. The CCM had a smooth surface with a WCA of $92.4 \pm 0.8^\circ$ (Figure 4a). After etching by a mixed aqueous solution of 0.13 M ammonium persulfate and 2.5 M sodium hydroxide, the ECM surface became rough and many micronano sheet structures appeared. The ECM showed hydrophilicity with a WCA of $63.0 \pm 0.7^\circ$ (Figure 4b). The surface of the copper mesh modified with 1-dodecanethiol displayed numerous convex nanoclusters. The SCM surface exhibited superhydrophobic and superoleophilic characteristics, with a WCA of $155.1 \pm 1.8^\circ$ and an OCA of 0° (Figure 4c), due to the rough nanostructures and hydrophobic groups.

3.3. Oil–Water Separation. **3.3.1. Mechanism of Oil–Water Separation.** The oil–water separation performance of the SCM is evaluated by a separation experiment using a peanut oil–water mixture. Figure 5 shows the separation process of the peanut oil–water mixture (initial peanut oil volume and water volume were 30 and 170 mL, respectively) with a stirring speed of 700 rpm and a mesh aperture diameter of 180 μm . Figure 5a shows the oil–water separation device. When the peanut oil–water mixture was added to the oil–water separator, as shown in Figure 5b, the peanut oil passed through the SCM under centrifugation and flowed into the measuring cylinder through the oil collecting funnel. The water was intercepted in the separator, as shown in Figure 5c–e. Figure 5f shows the peanut oil collected in the measuring cylinder after separation.

To investigate the separation mechanism of the oil–water centrifugal separation device, the mechanism analysis was as follows.

Under the centrifugation, the liquid on the wall of the separator was affected by outward additional pressure, as shown in eq 1.

$$\Delta p_1 = \frac{\rho \omega^2 D^2}{4} \quad (1)$$

where Δp_1 is the additional pressure (Pa) upon centrifugation, ρ is the liquid density (kg m^{-3}), ω is the stirring speed (rpm), and D is the diameter (m) of the separator.

According to the capillarity model, when the liquid contacted the SCM, the intrusion pressure Δp_2 was generated by surface tension, as shown in eq 2:⁴⁴

$$\Delta p_2 = \frac{4\gamma \cos \theta}{d} \quad (2)$$

where Δp_2 is the intrusion pressure (Pa) caused by surface tension, γ is the surface tension (N m^{-1}), θ is the contact angle (deg) between the liquid droplet and the SCM, and d is the SCM aperture diameter (m).

According to eq 2, the direction of Δp_2 is related to θ . For oil, $\theta_{\text{OCA}} < 90^\circ$ (θ_{OCA} is the contact angle between oil and the SCM), Δp_2 and Δp_1 are in the same direction so the oil can spontaneously penetrate the SCM. For water, $\theta_{\text{WCA}} > 90^\circ$ (θ_{WCA} is the contact angle between water and SCM), so Δp_2

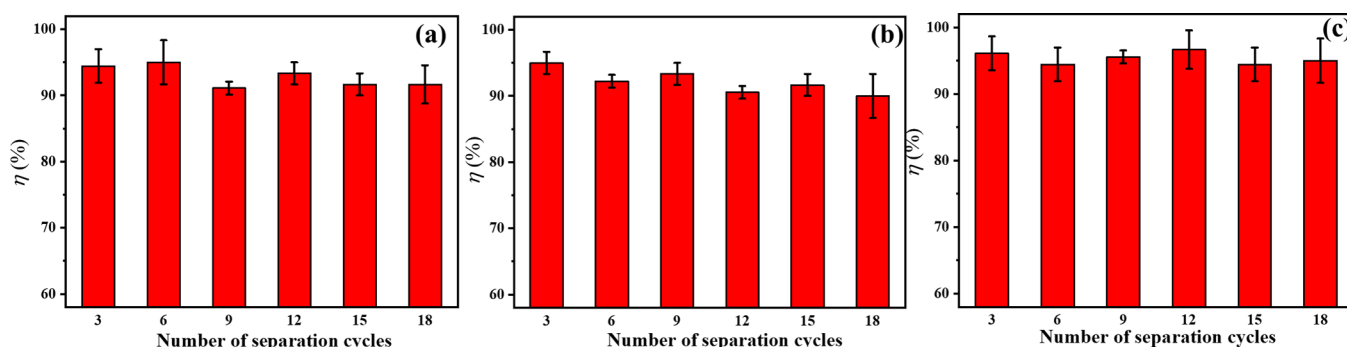


Figure 10. Separation efficiencies of various edible oil–water mixtures with different numbers of separation cycles for (a) sunflower seed oil, (b) corn oil, and (c) peanut oil.

and Δp_1 are in opposite directions (Figure 6). Thus, to separate the oil–water mixture, the water must be intercepted by the SCM. The relationship between Δp_1 and Δp_2 of water should satisfy eq 3:

$$\frac{\rho_w \omega^2 D^2}{4} \leq -\frac{4\gamma_w \cos \theta_{WCA}}{d} \quad (3)$$

where ρ_w is the water density (kg m^{-3}), ω is the stirring speed (rpm), D is the diameter (m) of the separator, γ_w is the surface tension (N m^{-1}) of water, θ_{WCA} is the contact angle (deg) between the water and the SCM, and d is the SCM aperture diameter (m).

According to the experimental conditions shown in Table 1, when the stirring speed was 700 rpm, the theoretical maximum SCM aperture diameter for intercepting water was calculated by eq 3 as $d_{\text{max,th}} = 1320 \mu\text{m}$.

3.3.2. Effect of the SCM Aperture Diameter. The effect of the SCM aperture diameter on the separation of a peanut oil–water mixture (30 mL oil, 170 mL water) at a stirring speed of 700 rpm is shown in Figure 7. When the separation time was 10 min, the volume of the separated phase with an SCM aperture diameter of 600, 300, 180, and 125 μm was 37.0, 35.0, 25.0, and 18.0 mL, respectively, and at the end of separation, the volume of the separated phase was 41.5, 38.5, 30.0, and 29.0 mL, respectively. When the SCM aperture diameter was $>180 \mu\text{m}$, the separation phase was mixed with water, as shown in the photographs of the separation phase in Figure 7. These results showed that the experimental maximum SCM aperture diameter for intercepting the water was 180 μm at a stirring speed of 700 rpm, which was less than the theoretical maximum SCM aperture diameter (1320 mm). This could have been because water was brought out when the oil penetrated the SCM due to the water-in-oil fluid in the mixture.

3.3.3. Effect of Stirring Speed. The effect of stirring speed on the separation of a peanut oil–water mixture (30 mL of oil, 170 mL of water) with an SCM aperture diameter of 180 μm is shown in Figure 8. When the separation time was 10 min, the volume of the separation phase at a stirring speed of 300, 500, 700, and 900 rpm was 5.5, 12.5, 25.0, and 31.0 mL, respectively, while at the end of separation, the volume of the separation phase was 13.0, 21.5, 30.0, and 42.0 mL, respectively. When the stirring speed was greater than 700 rpm, as can be seen from the photographs of the separation phase in Figure 8, the separation phase was mixed with water. The results showed that, when the stirring speed was less than 700 rpm, the oil–water separation was effective due to the

additional water pressure under the centrifugation being less than the intrusion pressure. However, the oil output was low because of the insufficient centrifugal speed.

3.3.4. Separation Efficiency of Edible Oil–Water Mixture. Based on the discussion in Sections 3.3.2 and 3.3.3, the separation efficiency for different edible oil–water mixtures with a stirring speed of 700 rpm and SCM aperture diameter of 180 μm was studied. The separation efficiency of oil–water mixture η was defined as eq 4:

$$\eta = \frac{V_L}{V_0} \times 100\% \quad (4)$$

where η is the oil–water separation efficiency, V_0 is the initial volume (mL) of the oil in the oil–water mixture, and V_L is the volume (mL) of liquid in the graduated cylinder at different times.

Figure 9 shows the separation efficiency of various edible oil–water mixtures (30 mL of oil, 170 mL of water) with a stirring speed of 700 rpm and a mesh aperture diameter of 180 μm . When the separation time was 30 min, the separation was complete. At this time, the separation efficiency for the sunflower seed oil–water mixture, corn oil–water mixture, and peanut oil–water mixture was 96.7, 93.3, and 98.3%, respectively, and there was little water in the graduated cylinder. These results showed that the separation of edible oil–water mixtures by the SCM-based oil–water centrifugal separation device was efficient and rapid. There were minor differences in the separation efficiency of the three edible oil–water mixtures due to the different densities, surface tensions, viscosities, and other physical properties of the oils.³⁰

To study the stability of the SCM, the effect of cycle number on the separation efficiency of the three edible oil–water mixtures was investigated (Figure 10). The separation efficiency of the (a) sunflower seed oil–water mixture, (b) corn oil–water mixture, and (c) peanut oil–water mixture was greater than 90% after 18 separation cycles. This result indicated that SCM had stable superhydrophobicity and superoleophilicity.

4. CONCLUSIONS

A novel oil–water centrifugal separation device was designed by using a self-prepared SCM with a WCA of $155.1 \pm 1.8^\circ$ and an OCA of 0° . First, the SCM was characterized in detail. Then, its performance was tested using three edible oil–water mixtures. With a stirring speed of 700 rpm and an SCM aperture diameter of 180 μm , the separation efficiency of the sunflower seed oil–water mixture, corn oil–water mixture, and

peanut oil–water mixture by the separation device at 30 min was 96.7, 93.3, and 98.3%, respectively. Furthermore, the separation efficiency was still over 90% after 18 separation cycles for these three edible oil–water mixtures. It proved that the self-prepared SCM had excellent stability. Finally, a model was established to analyze the separation mechanism. The SCM-based oil–water centrifugal separation device holds promising application prospects for the solution of oily wastewater pollution.

AUTHOR INFORMATION

Corresponding Authors

Fengzhen Zhang – School of Chemical Engineering, Sichuan University of Science & Engineering, Zigong 643000, China; Email: zhangfengzhen421@163.com

Aiai Zhang – School of Chemical Engineering, Sichuan University of Science & Engineering, Zigong 643000, China; orcid.org/0009-0008-1572-0517; Email: zhangaiyai@suse.edu.cn

Authors

Ranhao Wu – School of Chemical Engineering, Sichuan University of Science & Engineering, Zigong 643000, China

Huanhuan Zhang – School of Chemical Engineering, Sichuan University of Science & Engineering, Zigong 643000, China

Yuling Ye – School of Chemical Engineering, Sichuan University of Science & Engineering, Zigong 643000, China; National Engineering Laboratory of Circular Economy, Sichuan University of Science and Engineering, Zigong 643000, China; Sichuan Engineering Technology Research Center for High Salt Wastewater Treatment and Resource Utilization, Sichuan University of Science and Engineering, Zigong 643000, China

Zhong Chen – Chongqing Institute of Green and Intelligent Technology, Chinese Academy of Sciences, Chongqing 400714, China; orcid.org/0000-0001-7632-9361

Complete contact information is available at: <https://pubs.acs.org/10.1021/acsomega.3c10436>

Author Contributions

[†]These authors contributed equally to this work.

Notes

The authors declare no competing financial interest.

ACKNOWLEDGMENTS

This study was partially supported by the National Natural Science Foundation of China (21868014 and 22108268); the Vanadium and Titanium Resources Utilization Key Laboratory of Sichuan Province (2018FTSZ21); the Sichuan Provincial Natural Science Foundation (2022YFG0134 and 2023NSFSC0847); the Scientific Research and Innovation Team Program of Sichuan University of Science and Technology (SUSE652A003).

REFERENCES

- (1) Lee, Z. S.; Chin, S. Y.; Lim, J. W.; Witoon, T.; Cheng, C. K. Treatment Technologies of Palm Oil Mill Effluent (POME) and Olive Mill Wastewater (OMW): A Brief Review. *Environ. Technol. Inno.* **2019**, *15*, No. 100377.
- (2) Ngoie, W. I.; Oyekola, O. O.; Ikhu-omogbe, D.; Welz, P. J. Valorisation of Edible Oil Wastewater Sludge: Bioethanol and Biodiesel Production. *Waste Biomass Valori.* **2020**, *11*, 2431–2440.
- (3) Iskandar, M. J.; Baharum, A.; Anuar, F. H.; Othaman, R. Palm Oil Industry in South East Asia and the Effluent Treatment Technology-A Review. *Environ. Technol. Inno.* **2018**, *9*, 169–185.
- (4) Sanghamitra, P.; Mazumder, D.; Mukherjee, S. Treatment of Wastewater Containing Oil and Grease by Biological Method-A Review. *J. Environ. Sci. Heal. A* **2021**, *56*, 394–412.
- (5) Elanchezhian, S. S. D.; Meenakshi, S. Facile Fabrication of Metal Ions-Incorporated Chitosan/ β -Cyclodextrin Composites for Effective Removal of Oil from Oily Wastewater. *ChemistrySelect* **2017**, *2*, 11393–11401.
- (6) Younker, J. M.; Walsh, M. E. Effect of Adsorbent Addition on Floc Formation and Clarification. *Water Res.* **2016**, *98*, 1–8.
- (7) Zhao, C. L.; Zhou, J. Y.; Yan, Y.; Yang, L. W.; Xing, G. H.; Li, H. Y.; Wu, P.; Wang, M. Y.; Zheng, H. L. Application of Coagulation/Flocculation in Oily Wastewater Treatment: A Review. *Sci. Total Environ.* **2021**, *765*, No. 142795.
- (8) Daud, N. M.; Sheikh abdullah, S. R.; Abu hasan, H. Response Surface Methodological Analysis for the Optimization of Acid-Catalyzed Transesterification Biodiesel Wastewater Pre-treatment Using Coagulation-Flocculation Process. *Process Saf. Environ.* **2018**, *113*, 184–192.
- (9) Changmai, M.; Pasawan, M.; Purkait, M. K. Treatment of Oily Wastewater from Drilling Site Using Electrocoagulation Followed by Microfiltration. *Sep. Purif. Technol.* **2019**, *210*, 463–472.
- (10) Khalifa, O.; Banat, F.; Srinivasakannan, C.; Radjenovic, J.; Hasan, S. W. Performance Tests and Removal Mechanisms of Aerated Electrocoagulation in the Treatment of Oily Wastewater. *J. Water Process Eng.* **2020**, *36*, No. 101290.
- (11) Zhang, H.; Duan, M.; Fang, S. W.; Zhai, L.; Wang, X. J. Preparation of a Novel Flocculant and Its Performance for Treating Acidic Oily Wastewater. *RSC Advances.* **2016**, *6*, 106102–106108.
- (12) Sharma, S.; Simsek, H. Treatment of Canola-Oil Refinery Effluent Using Electrochemical Methods: A Comparison between Combined Electrocoagulation + Electrooxidation and Electrochemical Peroxidation Methods. *Chemosphere.* **2019**, *221*, 630–639.
- (13) Pitás, V.; Somogyi, V.; Kárpáti, A.; Thury, P.; Fráter, T. Reduction of Chemical Oxygen Demand in a Conventional Activated Sludge System Treating Coke Oven Wastewater. *J. Clean. Prod.* **2020**, *273*, No. 122482.
- (14) Li, J. H.; Sun, S. S.; Yan, P.; Fang, L.; Yu, Y.; Xiang, Y. D.; Wang, D.; Gong, Y. J.; Gong, Y. J.; Zhang, Z. Z. Microbial Communities in the Functional Areas of a Biofilm Reactor with Anaerobic-Aerobic Process for Oily Wastewater Treatment. *Bioresour. Technol.* **2017**, *238*, 7–15.
- (15) Morgan-sagastume, F.; Jacobsson, S.; Olsson, L. E.; Carlsson, M.; Gyllenhammar, M.; Sárvári horváth, I. Anaerobic Treatment of Oil-Contaminated Wastewater with Methane Production Using Anaerobic Moving Bed Biofilm Reactors. *Water Res.* **2019**, *163*, No. 114851.
- (16) González-gonzález, A.; Cuadros, F. Effect of Aerobic Pretreatment on Anaerobic Digestion of Olive Mill Wastewater (OMWW): An Ecoefficient Treatment. *Food Bioprod. Process.* **2015**, *95*, 339–345.
- (17) Qian, X. J.; Tang, T.; Wang, H.; Chen, C. G.; Luo, J. H.; Luo, D. L. Fabrication of Hydrophobic Ni Surface by Chemical Etching. *Materials* **2019**, *12*, 3546.
- (18) Tuo, Y. J.; Zhang, H. F.; Rong, W. T.; Jiang, S. Y.; Chen, W. P.; Liu, X. W. Drag Reduction of Anisotropic Superhydrophobic Surfaces Prepared by Laser Etching. *Langmuir* **2019**, *35*, 11016–11022.
- (19) Bi, P.; Li, H. L.; Zhao, G. C.; Ran, M. R.; Cao, L. L.; Guo, H. J.; Xue, Y. P. Robust Super-Hydrophobic Coating Prepared by Electrochemical Surface Engineering for Corrosion Protection. *Coatings* **2019**, *9*, 452.
- (20) Wang, S. Q.; Xue, Y. P.; Ban, C. L.; Xue, Y. Y.; Taleb, A.; Jin, Y. Fabrication of Robust Tungsten Carbide Particles Reinforced CoNi Super-Hydrophobic Composite Coating by Electrochemical Deposition. *Surf. Coat. Technol.* **2020**, *385*, No. 125390.
- (21) Huang, J. D.; Cai, P. H.; Li, M. M.; Wu, Q.; Li, Q.; Wang, S. Q. Preparation of CNF/PDMS Superhydrophobic Coatings with Good

- Abrasion Resistance Using a One-Step Spray Method. *Materials* **2020**, *13*, 5380.
- (22) Liu, X.; Chen, K.; Zhang, D. K.; Guo, Z. G. Stable and Durable Conductive Superhydrophobic Coatings Prepared by Double-Layer Spray Coating Method. *Nanomaterials* **2021**, *11*, 1506.
- (23) Wan, Y. X.; Chen, M. J.; Liu, W.; Shen, X. X.; Min, Y. L.; Xu, Q. J. The Research on Preparation of Superhydrophobic Surfaces of Pure Copper by Hydrothermal Method and Its Corrosion Resistance. *Electrochim. Acta* **2018**, *270*, 310–318.
- (24) Shayesteh, H.; Norouzebeigi, R.; Rahbar-kelishami, A. Hydrothermal Facile Fabrication of Superhydrophobic Magnetic Nanospiky Nickel Wires: Optimization Via Statistical Design. *Surf. Interfaces* **2021**, *26*, No. 101315.
- (25) Maurer, J. A.; Miller, M. J.; Bartolucci, S. F. Self-Cleaning Superhydrophobic Nanocomposite Surfaces Generated by Laser Pulse Heating. *J. Colloid Interface Sci.* **2018**, *524*, 204–208.
- (26) Liu, Y.; Zhang, K. T.; Yao, W. G.; Zhang, C. C.; Han, Z. W.; Ren, L. Q. A Facile Electrodeposition Process for the Fabrication of Superhydrophobic and Superoleophilic Copper Mesh for Efficient Oil-Water Separation. *Ind. Eng. Chem. Res.* **2016**, *55*, 2704–2712.
- (27) Zhang, J. C.; Liu, J. Y.; Wang, G. S.; Huang, L.; Chen, F. Z.; Liu, X. Controllable Wettability of Laser Treated Aluminum Mesh for On-Demand Oil/Water Separation. *J. Dispersion Sci. Technol.* **2019**, *40*, 1627–1636.
- (28) Qiao, X. Y.; Yang, C. Y.; Zhang, Q.; Yang, S. K.; Chen, Y. Y.; Zhang, D.; Yuan, X. Y.; Wang, W. K.; Zhao, Y. Q. Preparation of Parabolic Superhydrophobic Material for Oil-Water Separation. *Materials* **2018**, *11*, 1914.
- (29) Lee, C. H.; Johnson, N.; Drelich, J.; Yap, Y. K. The Performance of Superhydrophobic and Superoleophilic Carbon Nanotube Meshes in Water-Oil Filtration. *Carbon* **2011**, *49*, 669–676.
- (30) Zhu, D.; Tan, X.; Ji, L.; Shi, Z.; Zhang, X. Preparation of Transparent and Hydrophobic Cerium Oxide Films with Stable Mechanical Properties by Magnetron Sputtering. *Vacuum* **2021**, *184*, 109888–109896.
- (31) Shi, Z.; Zhou, Z.; Shum, P.; Li, L. K.-Y. Thermal Stability, Wettability and Corrosion Resistance of Sputtered Ceria Films on 316 Stainless Steel. *Appl. Surf. Sci.* **2019**, *477*, 166–171.
- (32) Zhu, D.; Shi, Z.; Tan, X.; Zhang, J.; Zhang, S.; Zhang, X. Accelerated Wetting Transition from Hydrophilic to Hydrophobic of Sputtered Cu Films with Micro-Scale Patterns. *Appl. Surf. Sci.* **2020**, *527*, 146741–146747.
- (33) Tan, X.; Zhu, D.; Shi, Z.; Zhang, X. Thickness-dependent Morphology, Microstructure, Adsorption and Surface Free Energy of Sputtered CeO₂ Films. *Ceram. Int.* **2020**, *46*, 13925–13931.
- (34) Zhu, D.; Liu, W.; Zhao, R.; Shi, Z.; Tan, X.; Zhang, Z.; Li, Y.; Ji, L.; Zhang, X. Microscopic Insights into Hydrophobicity of Cerium Oxide: Effects of Crystal Orientation and Lattice Constant. *J. Mater. Sci. Technol.* **2022**, *109*, 20–29.
- (35) Shi, Z.; Zeng, H.; Yuan, Y.; Shi, N.; Wen, L.; Rong, H.; Zhu, D.; Hu, L.; Ji, L.; Zhao, L.; Zhang, X. Constructing Superhydrophobicity by Self-Assembly of SiO₂@Polydopamine Core-Shell Nanospheres with Robust Oil-Water Separation Efficiency and Anti-Corrosion Performance. *Adv. Funct. Mater.* **2023**, *33*, 2213042–2213053.
- (36) Momeni, M. M.; Mirhosseini, M.; Nazari, Z.; Kazempour, A.; Hakimiyan, M. Antibacterial and Photocatalytic Activity of CuO Nanostructure Films with Different Morphology. *J. Mater. Sci-Mater. El.* **2016**, *27*, 8131–8137.
- (37) Chen, J. H.; Guo, D. Y.; Huang, C. Y.; Wen, X. F.; Xu, S. P.; Cheng, J.; Pi, P. H. Fabrication of Superhydrophobic Copper Mesh by Depositing CuCl for Oil/Water Separation. *Mater. Lett.* **2018**, *233*, 328–331.
- (38) Gao, R. X.; Liu, X.; Zhang, T. C.; Ouyang, L. K.; Liang, Y.; Yuan, S. J. Superhydrophobic Copper Foam Modified with n-Dodecyl Mercaptan-CeO₂ Nanosheets for Efficient Oil/Water Separation and Oil Spill Cleanup. *Ind. Eng. Chem. Res.* **2020**, *59*, 21510–21521.
- (39) Wang, K. F.; Lv, M. R.; Si, T.; Tang, X. N.; Wang, H.; Chen, Y. Y. Mechanism analysis of surface structure-regulated Cu₂O in photocatalytic antibacterial process. *J. Hazard. Mater.* **2024**, *461*, No. 132479.
- (40) Guo, X. L.; Wang, C.; Yang, Z. H.; Yang, Y. Boosting C₂₊ production from photoelectrochemical CO₂ reduction on gallium doped Cu₂O. *Chem. Eng. J.* **2023**, *471*, No. 144539.
- (41) Zhao, C.; Fu, H. T.; Yang, X. H.; Xiong, S. X.; Han, D. Z.; An, X. Z. Adsorption and photocatalytic performance of Au nanoparticles decorated porous Cu₂O nanospheres under simulated solar light irradiation. *Appl. Surf. Sci.* **2021**, *545*, No. 149014.
- (42) Pan, Q. M.; Wang, M.; Wang, H. B. Separating Small Amount of Water and Hydrophobic Solvents by Novel Superhydrophobic Copper Meshes. *Appl. Surf. Sci.* **2008**, *254*, 6002–6006.
- (43) Liu, X. L.; Jiang, Z. H.; Li, J.; Zhang, Z. H.; Ren, L. Q. Super-Hydrophobic Property of Nano-Sized Cupric Oxide Films. *Surf. Coat. Technol.* **2010**, *204*, 3200–3204.
- (44) Li, Q. Q.; Deng, W. J.; Li, C. H.; Sun, Q. Y.; Huang, F. Z.; Zhao, Y.; Li, S. K. High-Flux Oil/Water Separation with Interfacial Capillary Effect in Switchable Superwetting Cu(OH)₂@ZIF-8 Nanowire Membranes. *ACS Appl. Mater. Interfaces* **2018**, *10*, 40265–40273.